Test of CP Symmetry in the Neutral Decays of Λ via $J/\psi \to \Lambda\bar{\Lambda}$

M. Ablikim[1], M. N. Achasov[4,c], P. Adlarson[80], X. C. Ai[85], R. Aliberti[37], A. Amoroso[79A,79C], Q. An[76,62,†], Y. Bai[60], O. Bakina[38], Y. Ban[48,h], H.-R. Bao[68], V. Batozskaya[1,46], K. Begzsuren[34], N. Berger[37], M. Berlowski[46], M. B. Bertani[29A], D. Bettoni[30A], F. Bianchi[79A,79C], E. Bianco[79A,79C], A. Bortone[79A,79C], I. Boyko[38], R. A. Briere[5], A. Brueggemann[73], H. Cai[81], M. H. Cai[40,k,l], X. Cai[1,62], A. Calcaterra[29A], G. F. Cao[1,68], N. Cao[1,68], S. A. Cetin[66A], X. Y. Chai[48,h], J. F. Chang[1,62], T. T. Chang[45], G. R. Che[45], Y. Z. Che[1,62,68], C. H. Chen[9], Chao Chen[58], G. Chen[1], H. S. Chen[1,68], H. Y. Chen[20], M. L. Chen[1,62,68], S. J. Chen[44], S. M. Chen[65], T. Chen[1,68], X. R. Chen[33,68], X. T. Chen[1,68], X. Y. Chen[11,g], Y. B. Chen[1,62], Y. Q. Chen[15], Z. K. Chen[63], J. C. Cheng[47], L. N. Cheng[45], S. K. Choi[10], X. Chu[11,g], G. Cibinetto[30A], F. Cossio[79C], J. Cottee-Meldrum[67], H. L. Dai[1,62], J. P. Dai[83], X. C. Dai[65], A. Dbeyssi[18], R. E. de Boer[3], D. Dedovich[38], C. Q. Deng[77], Z. Y. Deng[1], A. Denig[37], I. Denisenko[38], M. Destefanis[79A,79C], F. De Mori[79A,79C], X. X. Ding[48,h], Y. Ding[42], Y. X. Ding[31], J. Dong[1,62], L. Y. Dong[1,68], M. Y. Dong[1,62,68], X. Dong[81], M. C. Du[1], S. X. Du[85], S. X. Du[11,g], X. L. Du[85], Y. Y. Duan[58], Z. H. Duan[44], P. Egorov[38,b], G. F. Fan[44], J. J. Fan[19], Y. H. Fan[47], J. Fang[1,62], J. Fang[63], S. S. Fang[1,68], W. X. Fang[1], Y. Q. Fang[1,62,†], L. Fava[79B,79C], F. Feldbauer[3], G. Felici[29A], C. Q. Feng[76,62], J. H. Feng[15], L. Feng[40,k,l], Q. X. Feng[40,k,l], Y. T. Feng[76,62], M. Fritsch[3], C. D. Fu[1], J. L. Fu[68], Y. W. Fu[1,68], H. Gao[68], Y. Gao[76,62], Y. N. Gao[48,h], Y. N. Gao[19], Y. Y. Gao[31], Z. Gao[45], S. Garbolino[79C], I. Garzia[30A,30B], L. Ge[60], P. T. Ge[19], Z. W. Ge[44], C. Geng[63], E. M. Gersabeck[72], A. Gilman[74], K. Goetzen[12], J. D. Gong[36], L. Gong[42], W. X. Gong[1,62], W. Gradl[37], S. Gramigna[30A,30B], M. Greco[79A,79C], M. D. Gu[53], M. H. Gu[1,62], C. Y. Guan[1,68], A. Q. Guo[33], J. N. Guo[11,g], L. B. Guo[43], M. J. Guo[52], R. P. Guo[51], X. Guo[52], Y. P. Guo[11,g], A. Guskov[38,b], J. Gutierrez[28], T. T. Han[1], F. Hanisch[3], K. D. Hao[76,62], X. Q. Hao[19], F. A. Harris[70], C. Z. He[48,h], K. L. He[1,68], F. H. Heinsius[3], C. H. Heinz[37], Y. K. Heng[1,62,68], C. Herold[64], P. C. Hong[36], G. Y. Hou[1,68], X. T. Hou[1,68], Y. R. Hou[68], Z. L. Hou[1], H. M. Hu[1,68], J. F. Hu[59,j], Q. P. Hu[76,62], S. L. Hu[11,g], T. Hu[1,62,68], Y. Hu[1], Z. M. Hu[63], G. S. Huang[76,62], K. X. Huang[63], L. Q. Huang[33,68], P. Huang[44], X. T. Huang[52], Y. P. Huang[1], Y. S. Huang[63], T. Hussain[78], N. Hüsken[37], N. in der Wiesche[73], J. Jackson[28], Q. Ji[1], Q. P. Ji[19], W. Ji[1,68], X. B. Ji[1,68], X. L. Ji[1,62], X. Q. Jia[52], Z. K. Jia[76,62], D. Jiang[1,68], H. B. Jiang[81], P. C. Jiang[48,h], S. J. Jiang[9], X. S. Jiang[1,62,68], Y. Jiang[68], J. B. Jiao[52], J. K. Jiao[36], Z. Jiao[24], S. Jin[44], Y. Jin[71], M. Q. Jing[1,68], X. M. Jing[68], T. Johansson[80], S. Kabana[35], N. Kalantar-Nayestanaki[69], X. L. Kang[9], X. S. Kang[42], M. Kavatsyuk[69], B. C. Ke[85], V. Khachatryan[28], A. Khoukaz[73], O. B. Kolcu[66A], B. Kopf[3], L. Kröger[73], M. Kuessner[3], X. Kui[1,68], N. Kumar[27], A. Kupsc[46,80], W. Kühn[39], Q. Lan[77], W. N. Lan[19], T. T. Lei[76,62], M. Lellmann[37], T. Lenz[37], C. Li[49], C. Li[45], C. H. Li[43], C. K. Li[20], D. M. Li[85], F. Li[1,62], G. Li[1], H. B. Li[1,68], H. J. Li[19], H. L. Li[85], H. N. Li[59,j], Hui Li[45], J. R. Li[65], J. S. Li[63], J. W. Li[52], K. Li[1], K. L. Li[40,k,l], L. J. Li[1,68], Lei Li[50], M. H. Li[45], M. R. Li[1,68], P. L. Li[68], P. R. Li[40,k,l], Q. M. Li[1,68], Q. X. Li[52], R. Li[17,33], S. X. Li[11], Shanshan Li[26,i], T. Li[52], T. Y. Li[45], W. D. Li[1,68], W. G. Li[1,†], X. Li[1,68], X. H. Li[76,62], X. K. Li[48,h], X. L. Li[52], X. Y. Li[1,8], X. Z. Li[63], Y. Li[19], Y. G. Li[48,h], Y. P. Li[36], Z. H. Li[40], Z. J. Li[63], Z. X. Li[45], Z. Y. Li[83], C. Liang[44], H. Liang[76,62], Y. F. Liang[57], Y. T. Liang[33,68], G. R. Liao[13], L. B. Liao[63], M. H. Liao[63], Y. P. Liao[1,68], J. Libby[27], A. Limphirat[64], D. X. Lin[33,68], L. Q. Lin[41], T. Lin[1], B. J. Liu[1], B. X. Liu[81], C. X. Liu[1], F. Liu[1], F. H. Liu[56], Feng Liu[6], G. M. Liu[59,j], H. Liu[40,k,l], H. B. Liu[14], H. H. Liu[1], H. M. Liu[1,68], Huihui Liu[21], J. B. Liu[76,62], J. J. Liu[20], K. Liu[40,k,l], K. Liu[77], K. Y. Liu[42], Ke Liu[22], L. Liu[40], L. C. Liu[45], Lu Liu[45], M. H. Liu[36], P. L. Liu[1], Q. Liu[68], S. B. Liu[76,62], W. M. Liu[76,62], W. T. Liu[41], X. Liu[40,k,l], X. K. Liu[40,k,l], X. L. Liu[11,g], X. Y. Liu[81], Y. Liu[40,k,l], Y. Liu[85], Y. B. Liu[45], Z. A. Liu[1,62,68], Z. D. Liu[9], Z. Q. Liu[52], Z. Y. Liu[40], X. C. Lou[1,62,68], H. J. Lu[24], J. G. Lu[1,62], X. L. Lu[15], Y. Lu[7], Y. H. Lu[1,68], Y. P. Lu[1,62], Z. H. Lu[1,68], C. L. Luo[43], J. R. Luo[63], J. S. Luo[1,68], M. X. Luo[84], T. Luo[11,g], X. L. Luo[1,62], Z. Y. Lv[22], X. R. Lyu[68,o], Y. F. Lyu[45], Y. H. Lyu[85], F. C. Ma[42], H. L. Ma[1], Heng Ma[26,i], J. L. Ma[1,68], L. L. Ma[52], L. R. Ma[71], Q. M. Ma[1], R. Q. Ma[1,68], R. Y. Ma[19], T. Ma[76,62], X. T. Ma[1,68], X. Y. Ma[1,62], Y. M. Ma[33], F. E. Maas[18],

I. MacKay[74], M. Maggiora[79A,79C], S. Malde[74], Q. A. Malik[78], H. X. Mao[40,k,l], Y. J. Mao[48,h], Z. P. Mao[1], S. Marcello[79A,79C], A. Marshall[67], F. M. Melendi[30A,30B], Y. H. Meng[68], Z. X. Meng[71], G. Mezzadri[30A], H. Miao[1,68], T. J. Min[44], R. E. Mitchell[28], X. H. Mo[1,62,68], B. Moses[28], N. Yu. Muchnoi[4,c], J. Muskalla[37], Y. Nefedov[38], F. Nerling[18,e], H. Neuwirth[73], Z. Ning[1,62], S. Nisar[32,a], Q. L. Niu[40,k,l], W. D. Niu[11,g], Y. Niu[52], C. Normand[67], S. L. Olsen[10,68], Q. Ouyang[1,62,68], S. Pacetti[29B,29C], X. Pan[58], Y. Pan[60], A. Pathak[10], Y. P. Pei[76,62], M. Pelizaeus[3], H. P. Peng[76,62], X. J. Peng[40,k,l], Y. Y. Peng[40,k,l], K. Peters[12,e], K. Petridis[67], J. L. Ping[43], R. G. Ping[1,68], S. Plura[37], V. Prasad[36], F. Z. Qi[1], H. R. Qi[65], M. Qi[44], S. Qian[1,62], W. B. Qian[68], C. F. Qiao[68], J. H. Qiao[19], J. J. Qin[77], J. L. Qin[58], L. Q. Qin[13], L. Y. Qin[76,62], P. B. Qin[77], X. P. Qin[41], X. S. Qin[52], Z. H. Qin[1,62], J. F. Qiu[1], Z. H. Qu[77], J. Rademacker[67], C. F. Redmer[37], A. Rivetti[79C], M. Rolo[79C], G. Rong[1,68], S. S. Rong[1,68], F. Rosini[29B,29C], Ch. Rosner[18], M. Q. Ruan[1,62], N. Salone[46,p], A. Sarantsev[38,d], Y. Schelhaas[37], K. Schoenning[80], M. Scodeggio[30A], W. Shan[25], X. Y. Shan[76,62], Z. J. Shang[40,k,l], J. F. Shangguan[16], L. G. Shao[1,68], M. Shao[76,62], C. P. Shen[11,g], H. F. Shen[1,8], W. H. Shen[68], X. Y. Shen[1,68], B. A. Shi[68], H. Shi[76,62], J. L. Shi[11,g], J. Y. Shi[1], S. Y. Shi[77], X. Shi[1,62], H. L. Song[76,62], J. J. Song[19], M. H. Song[40], T. Z. Song[63], W. M. Song[36], Y. X. Song[48,h,m], Zirong Song[26,i], S. Sosio[79A,79C], S. Spataro[79A,79C], S. Stansilaus[74], F. Stieler[37], S. S Su[42], G. B. Sun[81], G. X. Sun[1], H. Sun[68], H. K. Sun[1], J. F. Sun[19], K. Sun[65], L. Sun[81], R. Sun[76], S. S. Sun[1,68], T. Sun[54,f], W. Y. Sun[53], Y. C. Sun[81], Y. H. Sun[31], Y. J. Sun[76,62], Y. Z. Sun[1], Z. Q. Sun[1,68], Z. T. Sun[52], C. J. Tang[57], G. Y. Tang[1], J. Tang[63], J. J. Tang[76,62], L. F. Tang[41], Y. A. Tang[81], L. Y. Tao[77], M. Tat[74], J. X. Teng[76,62], J. Y. Tian[76,62], W. H. Tian[63], Y. Tian[33], Z. F. Tian[81], I. Uman[66B], B. Wang[1], B. Wang[63], Bo Wang[76,62], C. Wang[40,k,l], C. Wang[19], Cong Wang[22], D. Y. Wang[48,h], H. J. Wang[40,k,l], J. Wang[9], J. J. Wang[81], J. P. Wang[52], K. Wang[1,62], L. L. Wang[1], L. W. Wang[36], M. Wang[52], M. Wang[76,62], N. Y. Wang[68], S. Wang[40,k,l], Shun Wang[61], T. Wang[11,g], T. J. Wang[45], W. Wang[63], W. P. Wang[37], X. Wang[48,h], X. F. Wang[40,k,l], X. L. Wang[11,g], X. N. Wang[1,68], Xin Wang[26,i], Y. Wang[1], Y. D. Wang[47], Y. F. Wang[1,8,68], Y. H. Wang[40,k,l], Y. J. Wang[76,62], Y. L. Wang[19], Y. N. Wang[47], Y. N. Wang[81], Yaqian Wang[17], Yi Wang[65], Yuan Wang[17,33], Z. Wang[1,62], Z. Wang[45], Z. L. Wang[2], Z. Q. Wang[11,g], Z. Y. Wang[1,68], Ziyi Wang[68], D. Wei[45], D. H. Wei[13], H. R. Wei[45], F. Weidner[73], S. P. Wen[1], U. Wiedner[3], G. Wilkinson[74], M. Wolke[80], J. F. Wu[1,8], L. H. Wu[1], L. J. Wu[1,68], L. J. Wu[19], Lianjie Wu[19], S. G. Wu[1,68], S. M. Wu[68], X. Wu[11,g], Y. J. Wu[33], Z. Wu[1,62], L. Xia[76,62], B. H. Xiang[1,68], D. Xiao[40,k,l], G. Y. Xiao[44], H. Xiao[77], Y. L. Xiao[11,g], Z. J. Xiao[43], C. Xie[44], K. J. Xie[1,68], Y. Xie[52], Y. G. Xie[1,62], Y. H. Xie[6], Z. P. Xie[76,62], T. Y. Xing[1,68], C. J. Xu[63], G. F. Xu[1], H. Y. Xu[2], M. Xu[76,62], Q. J. Xu[16], Q. N. Xu[31], T. D. Xu[77], X. P. Xu[58], Y. Xu[11,g], Y. C. Xu[82], Z. S. Xu[68], F. Yan[23], L. Yan[11,g], W. B. Yan[76,62], W. C. Yan[85], W. H. Yan[6], W. P. Yan[19], X. Q. Yan[1,68], H. J. Yang[54,f], H. L. Yang[36], H. X. Yang[1], J. H. Yang[44], R. J. Yang[19], Y. Yang[11,g], Y. H. Yang[44], Y. Q. Yang[9], Y. Z. Yang[19], Z. P. Yao[52], M. Ye[1,62], M. H. Ye[8,†], Z. J. Ye[59,j], Junhao Yin[45], Z. Y. You[63], B. X. Yu[1,62,68], C. X. Yu[45], G. Yu[12], J. S. Yu[26,i], L. W. Yu[11,g], T. Yu[77], X. D. Yu[48,h], Y. C. Yu[85], Y. C. Yu[40], C. Z. Yuan[1,68], H. Yuan[1,68], J. Yuan[36], J. Yuan[47], L. Yuan[2], M. K. Yuan[11,g], S. H. Yuan[77], Y. Yuan[1,68], C. X. Yue[41], Ying Yue[19], A. A. Zafar[78], F. R. Zeng[52], S. H. Zeng[67], X. Zeng[11,g], Yujie Zeng[63], Y. J. Zeng[1,68], Y. C. Zhai[52], Y. H. Zhan[63], Shunan Zhang[74], B. L. Zhang[1,68], B. X. Zhang[1,†], D. H. Zhang[45], G. Y. Zhang[19], G. Y. Zhang[1,68], H. Zhang[76,62], H. Zhang[85], H. C. Zhang[1,62,68], H. H. Zhang[63], H. Q. Zhang[1,62,68], H. R. Zhang[76,62], H. Y. Zhang[1,62], J. Zhang[63], J. J. Zhang[55], J. L. Zhang[20], J. Q. Zhang[43], J. S. Zhang[11,g], J. W. Zhang[1,62,68], J. X. Zhang[40,k,l], J. Y. Zhang[1], J. Z. Zhang[1,68], Jianyu Zhang[68], L. M. Zhang[65], Lei Zhang[44], N. Zhang[85], P. Zhang[1,8], Q. Zhang[19], Q. Y. Zhang[36], R. Y. Zhang[40,k,l], S. H. Zhang[1,68], Shulei Zhang[26,i], X. M. Zhang[1], X. Y. Zhang[52], Y. Zhang[1], Y. Zhang[77], Y. T. Zhang[85], Y. H. Zhang[1,62], Y. P. Zhang[76,62], Z. D. Zhang[1], Z. H. Zhang[1], Z. L. Zhang[36], Z. L. Zhang[58], Z. X. Zhang[19], Z. Y. Zhang[81], Z. Y. Zhang[45], Z. Z. Zhang[47], Zh. Zh. Zhang[19], G. Zhao[1], J. Y. Zhao[1,68], J. Z. Zhao[1,62], L. Zhao[1], L. Zhao[76,62], M. G. Zhao[45], S. J. Zhao[85], Y. B. Zhao[1,62], Y. L. Zhao[58], Y. X. Zhao[33,68], Z. G. Zhao[76,62], A. Zhemchugov[38,b], B. Zheng[77],

B. M. Zheng[36], J. P. Zheng[1,62], W. J. Zheng[1,68], X. R. Zheng[19], Y. H. Zheng[68,o], B. Zhong[43], C. Zhong[19], H. Zhou[37,52,n], J. Q. Zhou[36], S. Zhou[6], X. Zhou[81], X. K. Zhou[6], X. R. Zhou[76,62], X. Y. Zhou[41], Y. X. Zhou[82], Y. Z. Zhou[11,g], A. N. Zhu[68], J. Zhu[45], K. Zhu[1], K. J. Zhu[1,62,68], K. S. Zhu[11,g], L. Zhu[36], L. X. Zhu[68], S. H. Zhu[75], T. J. Zhu[11,g], W. D. Zhu[11,g], W. J. Zhu[1], W. Z. Zhu[19], Y. C. Zhu[76,62], Z. A. Zhu[1,68], X. Y. Zhuang[45], J. H. Zou[1], J. Zu[76,62]

(BESIII Collaboration)

[1] *Institute of High Energy Physics, Beijing 100049, People's Republic of China*
[2] *Beihang University, Beijing 100191, People's Republic of China*
[3] *Bochum Ruhr-University, D-44780 Bochum, Germany*
[4] *Budker Institute of Nuclear Physics SB RAS (BINP), Novosibirsk 630090, Russia*
[5] *Carnegie Mellon University, Pittsburgh, Pennsylvania 15213, USA*
[6] *Central China Normal University, Wuhan 430079, People's Republic of China*
[7] *Central South University, Changsha 410083, People's Republic of China*
[8] *China Center of Advanced Science and Technology, Beijing 100190, People's Republic of China*
[9] *China University of Geosciences, Wuhan 430074, People's Republic of China*
[10] *Chung-Ang University, Seoul, 06974, Republic of Korea*
[11] *Fudan University, Shanghai 200433, People's Republic of China*
[12] *GSI Helmholtzcentre for Heavy Ion Research GmbH, D-64291 Darmstadt, Germany*
[13] *Guangxi Normal University, Guilin 541004, People's Republic of China*
[14] *Guangxi University, Nanning 530004, People's Republic of China*
[15] *Guangxi University of Science and Technology, Liuzhou 545006, People's Republic of China*
[16] *Hangzhou Normal University, Hangzhou 310036, People's Republic of China*
[17] *Hebei University, Baoding 071002, People's Republic of China*
[18] *Helmholtz Institute Mainz, Staudinger Weg 18, D-55099 Mainz, Germany*
[19] *Henan Normal University, Xinxiang 453007, People's Republic of China*
[20] *Henan University, Kaifeng 475004, People's Republic of China*
[21] *Henan University of Science and Technology, Luoyang 471003, People's Republic of China*
[22] *Henan University of Technology, Zhengzhou 450001, People's Republic of China*
[23] *Hengyang Normal University, Hengyang 421001, People's Republic of China*
[24] *Huangshan College, Huangshan 245000, People's Republic of China*
[25] *Hunan Normal University, Changsha 410081, People's Republic of China*
[26] *Hunan University, Changsha 410082, People's Republic of China*
[27] *Indian Institute of Technology Madras, Chennai 600036, India*
[28] *Indiana University, Bloomington, Indiana 47405, USA*
[29] *INFN Laboratori Nazionali di Frascati, (A)INFN Laboratori Nazionali di Frascati, I-00044, Frascati, Italy; (B)INFN Sezione di Perugia, I-06100, Perugia, Italy; (C)University of Perugia, I-06100, Perugia, Italy*
[30] *INFN Sezione di Ferrara, (A)INFN Sezione di Ferrara, I-44122, Ferrara, Italy; (B)University of Ferrara, I-44122, Ferrara, Italy*
[31] *Inner Mongolia University, Hohhot 010021, People's Republic of China*
[32] *Institute of Business Administration, Karachi,*
[33] *Institute of Modern Physics, Lanzhou 730000, People's Republic of China*
[34] *Institute of Physics and Technology, Mongolian Academy of Sciences, Peace Avenue 54B, Ulaanbaatar 13330, Mongolia*
[35] *Instituto de Alta Investigación, Universidad de Tarapacá, Casilla 7D, Arica 1000000, Chile*
[36] *Jilin University, Changchun 130012, People's Republic of China*
[37] *Johannes Gutenberg University of Mainz, Johann-Joachim-Becher-Weg 45, D-55099 Mainz, Germany*
[38] *Joint Institute for Nuclear Research, 141980 Dubna, Moscow region, Russia*
[39] *Justus-Liebig-Universitaet Giessen, II. Physikalisches Institut, Heinrich-Buff-Ring 16, D-35392 Giessen, Germany*
[40] *Lanzhou University, Lanzhou 730000, People's Republic of China*
[41] *Liaoning Normal University, Dalian 116029, People's Republic of China*
[42] *Liaoning University, Shenyang 110036, People's Republic of China*

[43] Nanjing Normal University, Nanjing 210023, People's Republic of China
[44] Nanjing University, Nanjing 210093, People's Republic of China
[45] Nankai University, Tianjin 300071, People's Republic of China
[46] National Centre for Nuclear Research, Warsaw 02-093, Poland
[47] North China Electric Power University, Beijing 102206, People's Republic of China
[48] Peking University, Beijing 100871, People's Republic of China
[49] Qufu Normal University, Qufu 273165, People's Republic of China
[50] Renmin University of China, Beijing 100872, People's Republic of China
[51] Shandong Normal University, Jinan 250014, People's Republic of China
[52] Shandong University, Jinan 250100, People's Republic of China
[53] Shandong University of Technology, Zibo 255000, People's Republic of China
[54] Shanghai Jiao Tong University, Shanghai 200240, People's Republic of China
[55] Shanxi Normal University, Linfen 041004, People's Republic of China
[56] Shanxi University, Taiyuan 030006, People's Republic of China
[57] Sichuan University, Chengdu 610064, People's Republic of China
[58] Soochow University, Suzhou 215006, People's Republic of China
[59] South China Normal University, Guangzhou 510006, People's Republic of China
[60] Southeast University, Nanjing 211100, People's Republic of China
[61] Southwest University of Science and Technology, Mianyang 621010, People's Republic of China
[62] State Key Laboratory of Particle Detection and Electronics, Beijing 100049, Hefei 230026, People's Republic of China
[63] Sun Yat-Sen University, Guangzhou 510275, People's Republic of China
[64] Suranaree University of Technology, University Avenue 111, Nakhon Ratchasima 30000, Thailand
[65] Tsinghua University, Beijing 100084, People's Republic of China
[66] Turkish Accelerator Center Particle Factory Group, (A)Istinye University, 34010, Istanbul, Turkey; (B)Near East University, Nicosia, North Cyprus, 99138, Mersin 10, Turkey
[67] University of Bristol, H H Wills Physics Laboratory, Tyndall Avenue, Bristol, BS8 1TL, UK
[68] University of Chinese Academy of Sciences, Beijing 100049, People's Republic of China
[69] University of Groningen, NL-9747 AA Groningen, The Netherlands
[70] University of Hawaii, Honolulu, Hawaii 96822, USA
[71] University of Jinan, Jinan 250022, People's Republic of China
[72] University of Manchester, Oxford Road, Manchester, M13 9PL, United Kingdom
[73] University of Muenster, Wilhelm-Klemm-Strasse 9, 48149 Muenster, Germany
[74] University of Oxford, Keble Road, Oxford OX13RH, United Kingdom
[75] University of Science and Technology Liaoning, Anshan 114051, People's Republic of China
[76] University of Science and Technology of China, Hefei 230026, People's Republic of China
[77] University of South China, Hengyang 421001, People's Republic of China
[78] University of the Punjab, Lahore-54590, Pakistan
[79] University of Turin and INFN, (A)University of Turin, I-10125, Turin, Italy; (B)University of Eastern Piedmont, I-15121, Alessandria, Italy; (C)INFN, I-10125, Turin, Italy
[80] Uppsala University, Box 516, SE-75120 Uppsala, Sweden
[81] Wuhan University, Wuhan 430072, People's Republic of China
[82] Yantai University, Yantai 264005, People's Republic of China
[83] Yunnan University, Kunming 650500, People's Republic of China
[84] Zhejiang University, Hangzhou 310027, People's Republic of China
[85] Zhengzhou University, Zhengzhou 450001, People's Republic of China

[†] Deceased
[a] Also at Bogazici University, 34342 Istanbul, Turkey
[b] Also at the Moscow Institute of Physics and Technology, Moscow 141700, Russia
[c] Also at the Novosibirsk State University, Novosibirsk, 630090, Russia
[d] Also at the NRC "Kurchatov Institute", PNPI, 188300, Gatchina, Russia

[e] Also at Goethe University Frankfurt, 60323 Frankfurt am Main, Germany
[f] Also at Key Laboratory for Particle Physics, Astrophysics and Cosmology, Ministry of Education; Shanghai Key Laboratory for Particle Physics and Cosmology; Institute of Nuclear and Particle Physics, Shanghai 200240, People's Republic of China
[g] Also at Key Laboratory of Nuclear Physics and Ion-beam Application (MOE) and Institute of Modern Physics, Fudan University, Shanghai 200443, People's Republic of China
[h] Also at State Key Laboratory of Nuclear Physics and Technology, Peking University, Beijing 100871, People's Republic of China
[i] Also at School of Physics and Electronics, Hunan University, Changsha 410082, China
[j] Also at Guangdong Provincial Key Laboratory of Nuclear Science, Institute of Quantum Matter, South China Normal University, Guangzhou 510006, China
[k] Also at MOE Frontiers Science Center for Rare Isotopes, Lanzhou University, Lanzhou 730000, People's Republic of China
[l] Also at Lanzhou Center for Theoretical Physics, Lanzhou University, Lanzhou 730000, People's Republic of China
[m] Also at Ecole Polytechnique Federale de Lausanne (EPFL), CH-1015 Lausanne, Switzerland
[n] Also at Helmholtz Institute Mainz, Staudinger Weg 18, D-55099 Mainz, Germany
[o] Also at Hangzhou Institute for Advanced Study, University of Chinese Academy of Sciences, Hangzhou 310024, China
[p] Currently at Silesian University in Katowice, Chorzow, 41-500, Poland
(Dated: October 29, 2025)

Using $(10087 \pm 44) \times 10^6$ J/ψ events collected with the BESIII detector, a full angular distribution analysis is carried out on the process $J/\psi \to \Lambda\bar{\Lambda} \to n\pi^0\bar{p}\pi^+ + c.c.$ The decay parameters α_0 for $\Lambda \to n\pi^0$ and $\bar{\alpha}_0$ for $\bar{\Lambda} \to \bar{n}\pi^0$ are measured to be $0.668 \pm 0.007 \pm 0.002$ and $-0.677 \pm 0.007 \pm 0.003$, respectively, yielding the most precise test for CP symmetry of neutral decays of Λ, $A^0_{CP} = (\alpha_0 + \bar{\alpha}_0)/(\alpha_0 - \bar{\alpha}_0)$, to be $-0.006 \pm 0.007 \pm 0.002$. The ratios α_0/α_- and $\bar{\alpha}_0/\alpha_+$ are determined to be $0.884 \pm 0.013 \pm 0.006$ and $0.885 \pm 0.013 \pm 0.004$, where α_- and α_+ are the decay parameters of $\Lambda \to p\pi^-$ and $\bar{\Lambda} \to \bar{p}\pi^+$, respectively. The ratios, found to be smaller than unity by more than 5σ, confirm the presence of the $\Delta I = 3/2$ transition in the Λ and $\bar{\Lambda}$ decays, which is expected to improve the theoretical calculations for strong and weak phases, and A_{CP}, in hyperon decays. In all results, the first and second uncertainties are statistical and systematic, respectively.

The violation of the combined charge-conjugation (C) and parity (P) symmetries, known as CP violation, is a key ingredient in explaining the observed matter–antimatter asymmetry of the universe through baryogenesis [1]. Despite accommodating CP violation via the Kobayashi-Maskawa phase [2, 3],the Standard Model (SM) fails to explain the baryon asymmetry of the universe [4]. Its predicted CP violation is at least ten orders of magnitude too small. Experimental evidence for CP violation has been found in K [5], B [6, 7] and D [8] meson systems and the Λ_b^0 baryon system [9], all these measurements are consistent with the SM predictions. Therefore, to resolve the baryogenesis puzzle, additional sources of CP violation beyond the SM must be considered. Hyperon decays, in particular, provide a sensitive probe for such effects [10, 11].

In the nonleptonic decays of spin 1/2 hyperons, CP violation arises from the interference between parity-conserving (P-wave) and parity-violating (S-wave) amplitudes with differing CP-odd weak phases [12]. In these decays, the angular distribution of the daughter baryon is given by $1 + \alpha_Y \boldsymbol{P_Y} \cdot \hat{\boldsymbol{p}}_{\boldsymbol{d}}$, where α_Y is the hyperon decay parameter, $\boldsymbol{P_Y}$ is the hyperon polarization vector, and $\hat{\boldsymbol{p}}_{\boldsymbol{d}}$ is the unit vector along the daughter baryon momentum in the hyperon rest frame. A CP-odd asymmetry parameter is defined as $A_{CP} = (\alpha_Y + \alpha_{\bar{Y}})/(\alpha_Y - \alpha_{\bar{Y}})$, where α_Y and $\alpha_{\bar{Y}}$ denote the decay parameters of the hyperon and anti-hyperon, respectively. A nonzero A_{CP} indicates CP violation.

Within the SM, phenomenological studies based on different scenarios [10, 11, 13] predict an extremely small CP asymmetry in the Λ nonleptonic two-body weak decay, $|A^{\Lambda,\mathrm{SM}}_{CP}| \leq 3 \times 10^{-5}$. In contrast, several beyond SM theories predict significantly larger values, e.g. $|A^{\Lambda,\mathrm{MSM}}_{CP}| \leq 10^{-4}$ with minimal extensions of the SM (MSM) [14], $|A^{\Lambda,\mathrm{CMPC}}_{CP}| \leq 7\times10^{-4}$ with chromomagnetic-penguin contributions (CMPC) [15], $|A^{\Lambda,\mathrm{SUSY}}_{CP}| \leq 10^{-3}$ with supersymmetric models (SUSY) [16], and $|A^{\Lambda,\mathrm{DM}}_{CP}| \leq 1.6\times10^{-3}$ with dark matter models (DM) [17]. The main limitation in the precision of the theoretical predictions arises from the well known S/P-wave puzzle in hyperon nonleptonic decays, where the S- and P-wave amplitudes cannot be simultaneously described within leading-order chiral perturbation theory [18, 19]. Improved precision in the decay parameters can help resolve this puzzle. Such measurements can also sharpen the status of the

$\Delta I = 1/2$ rule in the spin 1/2 hyperon sector [20, 21], in comparison to kaon decays $K \to \pi\pi$ [22, 23] where the $\Delta I = 3/2$ transitions are strongly suppressed relative to the $\Delta I = 1/2$ ones [24, 25]. With increasing experimental precision, $\Delta I = 3/2$ contributions can no longer be neglected [26] and must be included in theoretical calculations of A_{CP}.

Recently, BESIII has performed a series of precision studies of nonleptonic two-body hyperon decays [26–33]. The decay parameters of the charged Λ decay mode $\Lambda \to p\pi^-$ (α_-) and $\bar{\Lambda} \to \bar{p}\pi^+$ (α_+) were measured with the highest precision in the decay sequence $J/\psi \to \Lambda(\to p\pi^-)\bar{\Lambda}(\to \bar{p}\pi^+)$ [28]. For the neutral decay modes of Λ, α_0 for $\Lambda \to n\pi^0$ and $\bar{\alpha}_0$ for $\bar{\Lambda} \to \bar{n}\pi^0$ were measured in the decay sequence $J/\psi \to \Xi^-\bar{\Xi}^+ \to \Lambda(\to n\pi^0)\pi^-\bar{\Lambda}(\to \bar{p}\pi^+)\pi^+$ and its charge conjugated channel [26]. $\bar{\alpha}_0$ was also measured in $J/\psi \to \Lambda(\to p\pi^-)\bar{\Lambda}(\to \bar{n}\pi^0)$ based on 1.3 billion J/ψ events [27], but its precision is poor due to limited statistics. However, the uncertainties in α_0 and $\bar{\alpha}_0$ remain substantially larger than those for the charged modes, motivating further improvement. The decay $J/\psi \to \Lambda(\to n\pi^0)\bar{\Lambda}(\to \bar{p}\pi^+)$ and its charge conjugated channel offer larger signal yields compared to the previous mode $J/\psi \to \Xi^-\bar{\Xi}^+$. Although the reduced quantum entanglement in this channel partly offsets the statistical advantage, it still provides a pathway toward more precise measurements of α_0 and $\bar{\alpha}_0$.

In this Letter, we present a full angular analysis of the decay $J/\psi \to \Lambda(\to n\pi^0)\bar{\Lambda}(\to \bar{p}\pi^+)$ and its charge conjugate, based on $(10087\pm44)\times10^6$ J/ψ events [34] collected with the BESIII detector. The transversely polarization of Λ and $\bar{\Lambda}$ together with their spin correlation, allow the angular distributions of both production and decay processes to be described by an extended helicity formalism [35]. Unless otherwise indicated, the $\bar{\Lambda} \to \bar{n}\pi^0$ mode is implicitly included throughout this text.

The BESIII experiment provides a unique platform to study hyperon production and decay properties in e^+e^- annihilation to a $\Lambda\bar{\Lambda}$ pair via the intermediate J/ψ resonance. The decay chain $J/\psi \to \Lambda(\to n\pi^0)\bar{\Lambda}(\to \bar{p}\pi^+)$ is characterized by five helicity angles $\xi = (\theta_\Lambda, \theta_n, \phi_n, \theta_{\bar{p}}, \phi_{\bar{p}})$ and the four parameters $\omega = (\alpha_{J/\psi}, \Delta\Phi, \alpha_0, \alpha_+)$, where θ_Λ is the polar angle of Λ in the center-of-mass (c.m.) system of J/ψ, and (θ_n, ϕ_n), $(\theta_{\bar{p}}, \phi_{\bar{p}})$ are the polar and azimuthal angles of the neutron and anti-proton in their respective rest frames, defined in a right-handed system [35]. The parameters $\alpha_{J/\psi}$ and $\Delta\Phi$ describe the production of $J/\psi \to \Lambda\bar{\Lambda}$, and α_0 and α_+ are the decay parameters of $\Lambda \to n\pi^0$ and $\bar{\Lambda} \to \bar{p}\pi^+$, respectively. The joint angular distribution of the decay is given by [35],

$$\begin{aligned}\mathcal{W}(\xi;\omega) = {}& \mathcal{F}_0(\xi) + \alpha_{J/\psi}\mathcal{F}_5(\xi) + \alpha_0\alpha_+[\mathcal{F}_1(\xi) \\ & + \sqrt{1-\alpha^2_{J/\psi}}\cos(\Delta\Phi)\mathcal{F}_2(\xi) - \alpha_{J/\psi}\mathcal{F}_6(\xi)] \\ & + \sqrt{1-\alpha^2_{J/\psi}}\sin(\Delta\Phi)[-\alpha_0\mathcal{F}_3 + \alpha_+\mathcal{F}_4],\end{aligned} \tag{1}$$

where the angular functions $\mathcal{F}_i(\xi)$ $(i = 0, 1, ..., 6)$ are described in Ref. [36]. In Eq. (1), the $\alpha_0\alpha_+$ terms arise from $\Lambda-\bar{\Lambda}$ spin correlations, while the α_0 and α_+ terms reflect the transverse polarization of Λ and $\bar{\Lambda}$, respectively.

Details of the BESIII detector are given in Refs. [37, 38]. The corresponding simulation, analysis framework, and software are presented in Refs. [39–41]. The Monte Carlo (MC) samples are generated with Geant4-based [42] software, which models the electron-positron collisions, particle decays, and detector response. A generic J/ψ MC sample, with statistics matching the data, is used to study the potential background contribution. To eliminate experimental bias, The analysis is performed blindly with central values hidden [43] until the procedure is finalized. Signal MC samples are used to validate the analysis approaches and to study the systematic effects.

Two oppositely charged tracks are detected in the main drift chamber (MDC). The $\bar{p}$ and π^+ candidates are primarily selected as in Ref. [44]. A discrepancy between data and MC simulation is observed in the $\bar{\Lambda}$ polar angle distribution, mainly due to the trigger efficiency in the endcap region. To minimize this effect, we require the absolute value of the cosine of the $\bar{p}$ polar angle must be less than 0.8. The $\bar{\Lambda}$ candidate is reconstructed from the $\bar{p}$ and π^+ tracks via a vertex fit [45], and its invariant mass must lie within five times its resolution, where the mass resolution is determined in bins of the $\bar{\Lambda}$ polar angle. The decay length of the reconstructed $\bar{\Lambda}$ is required to be positive. To suppress backgrounds from $J/\psi \to \Sigma^0\bar{\Sigma}^0$, $\Sigma^0\bar{\Lambda}$, $\gamma\Lambda\bar{\Lambda}$ and $\gamma\eta_c$, which include a $\bar{\Lambda}$ in their final state, we furthermore require $|M^{\rm rec}_{\bar{\Lambda}} - m_\Lambda| < 3\sigma^{\rm rec}_{\bar{\Lambda}}$. Here, $M^{\rm rec}_{\bar{\Lambda}} = \sqrt{(E_{\rm cm} - E_{\bar{\Lambda}})^2/c^4 - P^2_{\bar{\Lambda}}/c^2}$ is the recoiling mass of the $\bar{\Lambda}$, obtained from the c.m. energy $E_{\rm cm}$, as well as the energy $E_{\bar{\Lambda}}$ and momentum $P_{\bar{\Lambda}}$ of the $\bar{\Lambda}$ candidate from the vertex fit. The resolution $\sigma^{\rm rec}_{\bar{\Lambda}}$ is determined in bins of the $\bar{\Lambda}$ polar angle.

At least two photon candidates are required in the electromagnetic calorimeter (EMC). Neutral showers in the EMC are primarily selected as in Ref. [26]. To veto the showers from neutron (anti-neutron) interaction in the EMC, since the angle between neutron (anti-neutron) and $\Lambda(\bar{\Lambda})$ is very small (less than 7°), the photon candidates should be separated from the Λ $(\bar{\Lambda})$ momentum direction by more than 10° (15°), where the Λ $(\bar{\Lambda})$ momentum direction is opposite to that of $\bar{\Lambda}$ (Λ). To further suppress the neutron-induced shower, a boosted decision tree (BDT) classifier [46] is constructed using shower shape variables including deposited energy, number of hits, second moment, Zernike moments, and deposition shape [26]. Photons matched to truth information in signal MC are treated as signal, while others are treated as background. A requirement on the BDT output > 0.15 (0.10) is applied to ensure 90% signal efficiency, with a corresponding 55% (45%) background rejection efficiency. The π^0 candidates are reconstructed with a photon pair by performing a kinematic fit constraining their invariant mass to the π^0 nominal mass. In case of multiple π^0 candidates from combinatorial effects, the one with the smallest kinematic fit χ^2 is retained, requiring $\chi^2 < 100$.

Because of the limited detection efficiency for neutrons and antineutrons, they are not reconstructed directly. Instead, their four-momenta are inferred as $\boldsymbol{P}_n = \boldsymbol{P}_\Lambda - \boldsymbol{P}_{\pi^0}$, where $\boldsymbol{P}_n$, $\boldsymbol{P}_\Lambda$ and $\boldsymbol{P}_{\pi^0}$ are the four-momenta of neutron, Λ and π^0 candidate, respectively. To improve the resolution, the momentum and energy of Λ are set to $\vec{p}_\Lambda = -\hat{p}_{\bar{\Lambda}}\sqrt{E_{\rm cm}^2/c^2/4 - m_\Lambda^2 c^2}$ and $E_\Lambda = E_{\rm cm}/2$, respectively, where $\hat{p}_{\bar{\Lambda}}$ is the momentum direction of the $\bar{\Lambda}$ in the e^+e^- rest frame. The neutron is identified by the missing mass calculated from $\boldsymbol{P}_n$, which shows a clear peak near the nominal neutron mass with low background (Fig. 1). Studies of MC samples and data in the neutron sideband show that background in the signal region mainly arises from signal events with misreconstructed π^0 candidates, i.e., combinatorial background. The combinatorial background does not peak in the neutron invariant mass distribution. The other backgrounds, stemming from processes with one or two extra photons in the final state [47], contribute less than 0.5% and are neglected in the nominal analysis.

To extract the production and decay parameters, a simultaneous fit on the joint angular distribution is performed on the selected events in the neutron/antineutron missing-mass signal range $[0.926, 0.957]$ GeV/c^2, with the production parameters $\alpha_{J/\psi}$ and $\Delta\Phi$ shared between the two charge conjugated channels. In the fit, the probability density function for the i-th event with helicity angle ξ_i is parameterized with the four parameters ω,

$$\mathcal{P}(\xi_i;\omega) = \mathcal{W}(\xi_i;\omega)\varepsilon(\xi_i)/\mathcal{N}(\omega), \qquad (2)$$

where the normalization factor $\mathcal{N}(\omega)$ is obtained by $\mathcal{N}(\omega) = \frac{1}{M}\sum_{j=1}^{M}\frac{\mathcal{W}(\xi_j;\omega)}{\mathcal{W}(\xi_j;\omega_{\rm gen})}$ with a signal MC sample generated with known parameters $\omega_{\rm gen}$ [26, 28] and size M, similar to that in Ref. [26]. The sum runs over all M signal MC events, corresponding to 50 times the data yield. The log-likelihood function for N selected candidates is

$$\mathcal{S} = -\sum_{i=1}^{N}\ln\mathcal{P}(\xi_i;\omega) + \frac{N_{\rm bkg}}{N_{\rm miss}}\sum_{i}^{N_{\rm miss}}\ln\mathcal{P}(\xi_i;\omega), \qquad (3)$$

where the second term accounts for the contribution from the combinatorial background, estimated using $N_{\rm miss}$ MC-simulated background events. To determine the background yield $N_{\rm bkg}$, unbinned maximum likelihood fits are carried out on the distributions of the neutron missing mass, as shown in Fig. 1. In the fit, the signal is modeled with an MC-simulated shape convolved with a Gaussian function to account for the resolution difference between data and MC simulation, while the combinatorial background is modeled by the shape from the corresponding MC sample. The fit yields 872450 ± 982 signal events with a purity of 95.3% for the decay $\Lambda \to n\pi^0$, and 759770 ± 963 events with a purity of 91.1% for the decay $\bar{\Lambda} \to \bar{n}\pi^0$.

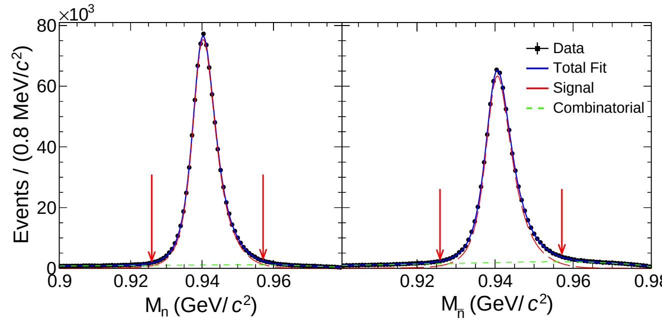

FIG. 1. Distributions of the missing masses for $\Lambda \to n\pi^0$ and $\bar{\Lambda} \to \bar{n}\pi^0$, respectively. The blue solid curve represents the total fit result. The red dashed and green dotted lines denote the signal shape and the combinatorial background contributions, respectively. The red arrows indicate the signal region.

The parameters ω are determined by a maximum likelihood fit, minimizing $\mathcal{S}$ with the TMinuit [48] package. The parameter $\alpha_{J/\psi}$ is fixed to the value reported in Ref. [28], a consequence of the data-MC discrepancy mentioned earlier. The fit results are summarized in Table I. The correlation coefficients are $\rho(\alpha_0, \bar{\alpha}_0) = -0.005$ and $\rho(\alpha_-, \alpha_+) = -0.026$. The moment μ, defined as

$$\mu(\cos\theta_\Lambda) = \frac{m}{N}\sum_{i=1}^{N_k}(\sin\theta_n^i \sin\phi_n^i + \sin\theta_{\bar{p}}^i \sin\phi_{\bar{p}}^i), \qquad (4)$$

is proportional to the product of the Λ polarization and its decay asymmetry. The quantity is evaluated across $m = 40$ bins in $\cos\theta_\Lambda$. For each bin k, containing N_k events, the index i denotes the i-th event within it. Comparison of the data with the phase-space (PHSP) MC sample reveals a significant polarization of the Λ hyperons in $J/\psi \to \Lambda\bar{\Lambda}$ decays, as shown in Fig. 2.

The sources of systematic uncertainties are separated into four categories: event reconstruction, background estimation, fit procedure and residual Data/MC discrepancy. For event reconstruction, the effects from p, $\bar{p}$, and $\pi^\pm$ tracking, PID, and $\Lambda/\bar{\Lambda}$ reconstruction are evaluated with a control sample of $J/\psi \to \Lambda(\to p\pi^-)\bar{\Lambda}(\to \bar{p}\pi^+)$. The π^0 reconstruction efficiency is studied with $J/\psi \to \Sigma^+(\to p\pi^0)\bar{\Sigma}^-(\to \bar{p}\pi^0)$, which has a final-state topology similar to the signal. Selection-related effects, such as the polar angle requirement of $\bar{p}$, the missing-mass window, and the χ^2 of the π^0 kinematic fit, are estimated by varying their values around the nominal ones and repeating the fits. Background-related uncertainties are evaluated in two ways: a $\pm 1\sigma$ variation of the combinatorial

TABLE I. Summaries of the production and decay parameters, the CP asymmetry $A_{CP}^{-} = (\alpha_- + \alpha_+)/(\alpha_- - \alpha_+)$ and $A_{CP}^{0} = (\alpha_0 + \bar{\alpha}_0)/(\alpha_0 - \bar{\alpha}_0)$, the average decay parameters $\langle\alpha_0\rangle = (\alpha_0 - \bar{\alpha}_0)/2$ and $\langle\alpha_-\rangle = (\alpha_- - \alpha_+)/2$, as well as the ratios α_0/α_- and $\bar{\alpha}_0/\alpha_+$. The first uncertainties are statistical and the second ones systematic.

Parameter	This work	Previous result
$\Delta\Phi$ (rad)	$0.748 \pm 0.006 \pm 0.004$	$0.7521 \pm 0.0042 \pm 0.0066$ [28]
α_-	$0.756 \pm 0.008 \pm 0.003$	$0.7519 \pm 0.0036 \pm 0.0024$ [28]
α_+	$-0.764 \pm 0.008 \pm 0.001$	$-0.7559 \pm 0.0036 \pm 0.0030$ [28]
α_0	$0.668 \pm 0.007 \pm 0.002$	$0.670 \pm 0.009^{+0.009}_{-0.008}$ [26]
$\bar{\alpha}_0$	$-0.677 \pm 0.007 \pm 0.003$	$-0.668 \pm 0.008^{+0.006}_{-0.008}$ [26]
A_{CP}^{-}	$-0.005 \pm 0.007 \pm 0.002$	$-0.0025 \pm 0.0046 \pm 0.0012$ [28]
A_{CP}^{0}	$-0.006 \pm 0.007 \pm 0.002$	$0.001 \pm 0.009^{+0.005}_{-0.007}$ [26]
$\langle\alpha_0\rangle$	$0.672 \pm 0.002 \pm 0.002$	$0.673 \pm 0.006^{+0.007}_{-0.006}$ [26]
$\langle\alpha_-\rangle$	$0.760 \pm 0.002 \pm 0.002$	$0.7542 \pm 0.0010 \pm 0.0024$ [28]
α_0/α_-	$0.884 \pm 0.013 \pm 0.006$	$0.877 \pm 0.015^{+0.014}_{-0.010}$ [26]
$\bar{\alpha}_0/\alpha_+$	$0.885 \pm 0.013 \pm 0.004$	$0.863 \pm 0.014^{+0.012}_{-0.008}$ [26]

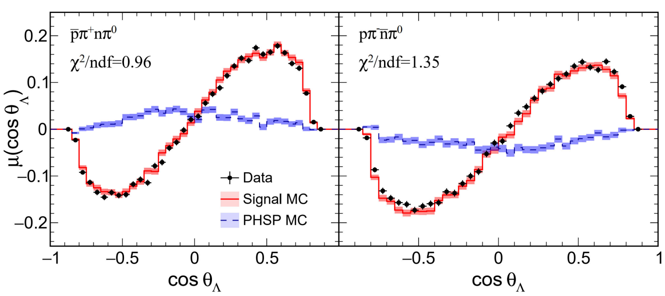

FIG. 2. Distributions of $\mu(\cos\theta_\Lambda)$ as a function of $\cos\theta_\Lambda$. The dots with error bars are data, the red solid lines are the signal MC sample and the blue dashed line represent the distributions without polarization from the PHSP MC sample. The red and blue bands indicate the statistical uncertainties of signal MC and PHSP MC samples, respectively.

background yield in the fit, and the inclusion of the dominant neglected background term, as determined from MC simulation, in an alternative fit. The uncertainty of fit procedure is tested with 50 sets of toy MC samples generated using the best-fit parameters. Since the input and output are consistent within statistical fluctuations, no additional uncertainty is assigned to the fit procedure. The fixed input of $\alpha_{J/\psi}$ is studied by repeating the fit with $\alpha_{J/\psi}$ randomly varied within one standard deviation for 100 iterations. The standard deviation of the output is assigned as the corresponding uncertainty. Finally, the residual data/MC discrepancy is evaluated by reweighting the MC to match the $\bar{\Lambda}$ polar-angle distribution in data; the shift in the fitted result is taken as the associated uncertainty. The absolute contributions from various sources are summarized in Table II. The total systematic uncertainty for each parameter is obtained by summing these individual contributions in quadrature.

Based on $(10087 \pm 44) \times 10^6$ J/ψ events collected with

TABLE II. Absolute systematic uncertainties of the measured parameters (in units of 10^{-3}). The "Event Reco", "Bkg Est", "Fit Meth" and "Data/MC Diff." represent the systematic uncertainty associated with event reconstruction, background estimation, fit method, and residual data/MC discrepancy, respectively.

Parameter	Event Reco	Bkg Est	Fit Meth	Data/MC Diff.	Total
$\Delta\Phi$ (rad)	1.3	2.7	2.3	2.1	4.3
α_-	1.9	1.8	0.3	0.9	2.8
α_+	0.9	0.7	0.3	0.3	1.2
α_0	1.6	0.4	0.6	0.6	1.9
$\bar{\alpha}_0$	2.4	0.4	0.6	2.0	3.2
A_{CP}^{-}	1.5	0.8	0.0	0.8	1.9
A_{CP}^{0}	2.0	0.1	0.1	1.0	2.2
$\langle\alpha_0\rangle$	1.1	0.4	0.6	1.3	1.9
$\langle\alpha_-\rangle$	0.9	1.2	0.3	0.3	1.6
α_0/α_-	5.0	2.7	0.5	1.8	5.9
$\bar{\alpha}_0/\alpha_+$	3.4	1.2	0.4	2.2	4.3

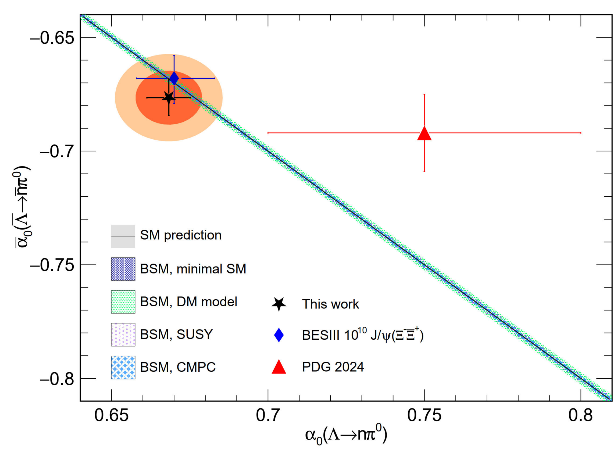

FIG. 3. Two dimensional distribution of the decay parameters $\bar{\alpha}_0$ versus α_0. The black star with error bars denotes the results measured in this work and the orange contours correspond to the 68%/95% confidence levels. The blue diamond shows the results of α_0 and $\bar{\alpha}_0$ by the process $J/\psi \to \Xi^-\bar{\Xi}^+$ with 10 billion J/ψ events [26]. The red triangle represents the PDG 2024 values [49]. The black line with gray band represents the prediction from the SM [13, 15]. The blue, green, violet and azure bands indicate the results predicted by minimal standard model [14], dark matter model [17], supersymmetry [16] and chromomagnetic-penguin contributions [15], respectively.

the BESIII detector, we perform a full angular analysis of the decay $J/\psi \to \Lambda(\to n\pi^0)\bar{\Lambda}(\to \bar{p}\pi^+)$ and its charge conjugated mode. The neutral decay parameters α_0 and $\bar{\alpha}_0$ are consistent with previous measurements [26, 27], with precisions improved by 43% and 27%, respectively, as shown in Fig. 3. This improvement is primarily reflected in the reduced systematic uncertainties. We also determine $\Delta\Phi$ and the charged decay parameters α_- and α_+, establishing nonzero polarization in $J/\psi \to \Lambda\bar{\Lambda}$, which are all consistent with the previous results [26–28, 30]. The derived CP asymmetries A^-_{CP} and A^0_{CP} are consistent with zero, with A^0_{CP} obtained at the highest precision to date (29% improvement). The ratios of the Λ decay parameters between the isospin conjugated decay modes α_0/α_- and $\bar{\alpha}_0/\alpha_+$, deviate from unity by 8.1σ and 8.5σ, respectively, confirming the $\Delta I = 3/2$ contributions. Combinning the averages of $\langle\alpha_0\rangle$, $\langle\alpha_-\rangle$, the decay rates $\Gamma(\Lambda \to p\pi^-)$, $\Gamma(\Lambda \to n\pi^0)$ [49] and the $N-\pi$ scattering phase shift [50], the ratio of $\Delta I = 3/2$ to $\Delta I = 1/2$ transitions in the S wave is determined to be $S_3/S_1 = 0.033 \pm 0.002 \pm 0.001 \pm 0.004$, and in the P wave to be $P_3/P_1 = -0.067 \pm 0.008 \pm 0.002 \pm 0.004$, in line with Ref.[10]. Here, the first uncertainties are statistical, the second systematic, and the third arise from the input parameters [49, 50]. The S-wave ratio agrees with $\mathrm{Re}(A_2)/\mathrm{Re}(A_0)$ in $K \to \pi\pi$ within the uncertainty, while the P-wave ratio shows a discrepancy. Building upon previous work [26], this analysis achieves the most precise measurement of neutral decays of Λ to date. It also demonstrates the necessity of including $\Delta I = 3/2$ amplitudes, and provide important benchmarks for future high-precision e^+e^- studies.

Acknowledgement

The BESIII Collaboration thanks the staff of BEPCII (https://cstr.cn/31109.02.BEPC), the IHEP computing center and the supercomputing center of the University of Science and Technology of China (USTC) for their strong support. This work is supported in part by National Key R&D Program of China under Contracts Nos. 2023YFA1606000, 2023YFA1606704, 2023YFA1609400; National Natural Science Foundation of China (NSFC) under Contracts Nos. 11635010, 11935015, 11935016, 11935018, 12025502, 12035009, 12035013, 12061131003, 12192260, 12192261, 12192262, 12192263, 12192264, 12192265, 12221005, 12225509, 12235017, 12361141819, 12122509, 12105276; the Chinese Academy of Sciences (CAS) Large-Scale Scientific Facility Program; the Strategic Priority Research Program of Chinese Academy of Sciences under Contract No. XDA0480600; CAS under Contract No. YSBR-101; 100 Talents Program of CAS; The Institute of Nuclear and Particle Physics (INPAC) and Shanghai Key Laboratory for Particle Physics and Cosmology; ERC under Contract No. 758462; German Research Foundation DFG under Contract No. FOR5327; Istituto Nazionale di Fisica Nucleare, Italy; Knut and Alice Wallenberg Foundation under Contracts Nos. 2021.0174, 2021.0299; Ministry of Development of Turkey under Contract No. DPT2006K-120470; National Research Foundation of Korea under Contract No. NRF-2022R1A2C1092335; National Science and Technology fund of Mongolia; Polish National Science Centre under Contract No. 2024/53/B/ST2/00975; STFC (United Kingdom); Swedish Research Council under Contract No. 2019.04595; U. S. Department of Energy under Contract No. DE-FG02-05ER41374. This paper is also supported by the Joint Large-Scale Scientific Facility Funds of the NSFC and CAS under Contracts Nos. U2032111; Beijing Natural Science Foundation of China (BNSF) under Contract No. IS23014.

[1] A. D. Sakharov, Pisma Zh. Eksp. Teor. Fiz. **5**, 32 (1967).
[2] N. Cabibbo, Phys. Rev. Lett. **10**, 531 (1963).
[3] M. Kobayashi and T. Maskawa, Prog. Theo. Phys. **49**, 652 (1973).
[4] S. Barr, G. Segrè, and H. A. Weldon, Phys. Rev. D **20**, 2494 (1979).
[5] J. H. Christenson, J. W. Cronin, V. L. Fitch, and R. Turlay, Phys. Rev. Lett. **13**, 138 (1964).
[6] B. Aubert *et al.* (BABAR Collaboration), Phys. Rev. Lett. **87**, 091801 (2001).
[7] K. Abe *et al.* (Belle Collaboration), Phys. Rev. Lett. **87**, 091802 (2001).
[8] R. Aaij *et al.* (LHCb Collaboration), Phys. Rev. Lett. **122**, 211803 (2019).
[9] R. Aaij *et al.* (LHCb), Nature **643**, 1223 (2025).
[10] N. Salone, P. Adlarson, V. Batozskaya, A. Kupsc, S. Leupold, and J. Tandean, Phys. Rev. D **105**, 116022 (2022).
[11] J. F. Donoghue, X.-G. He, and S. Pakvasa, Phys. Rev. D **34**, 833 (1986).
[12] T. D. Lee and C. N. Yang, Phys. Rev. **108**, 1645 (1957).
[13] J. Tandean and G. Valencia, Phys. Rev. D **67**, 056001 (2003).
[14] X.-G. He and G. Velencia, Phys. Rev. D **52**, 5257 (1995).
[15] X.-G. He, J. Tandean, and G. Valencia, Sci. Bull. **67**, 1840 (2022).
[16] X.-G. He, H. Murayama, S. Pakvasa, and G. Valencia, Phys. Rev. D **61**, 071701 (2000).
[17] X.-G. He, X.-D. Ma, J. Tandean, and G. Valencia, JHEP **07**, 078.
[18] E. E. Jenkins, Nucl. Phys. B **375**, 561 (1992).
[19] R.-X. Shi, S.-Y. Li, J.-X. Lu, and L.-S. Geng, Sci. Bull. **67**, 2298 (2022).
[20] O. E. Overseth and S. Pakvasa, Phys. Rev. **184**, 1663 (1969).
[21] S. Olsen, L. Pondrom, R. Handler, P. Limon, J. A. Smith, and O. E. Overseth, Phys. Rev. Lett. **24**, 843 (1970).
[22] A. Alavi-Harati *et al.* (KTeV Collaboration), Phys. Rev. Lett. **83**, 22 (1999).
[23] V. Fanti *et al.*, Phys. Lett. B **465**, 335 (1999).
[24] Y. Amhis *et al.* (Heavy Flavor Averaging Group Collaboration), Phys. Rev. D **107**, 052008 (2023).
[25] C. A. Manzari, A. M. Coutinho, and A. Crivellin, PoS **LHCP2020**, 242 (2021), arXiv:2009.03877 [hep-ph].
[26] M. Ablikim *et al.* (BESIII Collaboration), Phys. Rev. Lett. **132**, 101801 (2024).

[27] M. Ablikim *et al.* (BESIII), Nature Phys. **15**, 631 (2019).
[28] M. Ablikim *et al.* (BESIII Collaboration), Phys. Rev. Lett. **129**, 131801 (2022).
[29] M. Ablikim *et al.* (BESIII Collaboration), Nature **606**, 64 (2022).
[30] M. Ablikim *et al.* (BESIII Collaboration), Phys. Rev. D **108**, L031106 (2023).
[31] M. Ablikim *et al.* (BESIII Collaboration), Phys. Rev. Lett. **131**, 191802 (2023).
[32] M. Ablikim *et al.* (BESIII Collaboration), Phys. Rev. Lett. **133**, 101902 (2024).
[33] M. Ablikim *et al.* (BESIII Collaboration), Phys. Rev. D **108**, L091101 (2023).
[34] M. Ablikim *et al.* (BESIII Collaboration), Chin. Phys. C **46**, 074001 (2022).
[35] E. Perotti, G. Fäldt, A. Kupsc, S. Leupold, and J. J. Song, Phys. Rev. D **99**, 056008 (2019).
[36] G. Fäldt and A. Kupsc, Phys. Lett. B **772**, 16 (2017).
[37] M. Ablikim *et al.* (BESIII Collaboration), Nucl. Instrum. Meth. A **614**, 345 (2010).
[38] K.-X. Huang, Z.-J. Li, Z. Qian, J. Zhu, H.-Y. Li, Y.-M. Zhang, S.-S. Sun, and Z.-Y. You, Nucl. Sci. Tech. **33**, 142 (2022).
[39] R.-G. Ping, Chin. Phys. C **32**, 599 (2008).
[40] Z.-Y. Deng *et al.*, Chin. Phys. C **30**, 371 (2006).
[41] Y.-Z. Sun *et al.*, Hedianzixue Yu Tance Jishu/Nuclear Electronics and Detection Technology **27**, 842 (2007).
[42] S. Agostinelli *et al.* (GEANT4 Collaboration), Nucl. Instrum. Meth. A **506**, 250 (2003).
[43] J. R. Klein and A. Roodman, Ann. Rev. Nucl. Part. Sci. **55**, 141 (2005).
[44] M. Ablikim *et al.* (BESIII Collaboration), Phys. Rev. Lett. **129**, 212002 (2022).
[45] M. Xu, K.-L. He, Z.-P. Zhang, Y.-F. Wang, J.-M. Bian, C.-D. Fu, B. Huang, X.-B. Ji, S.-S. Sun, L. Yan, and J.-Y. Zhang, Chin. Phys. C **34**, 92 (2010).
[46] J. Therhaag, in *Proceedings of 35th International Conference of High Energy Physics — PoS(ICHEP 2010)*, ICHEP 2010 (Sissa Medialab, 2011) p. 510.
[47] X. Zhou, S. Du, G. Li, and C. Shen, Comp. Phy. Comm. **258**, 107540 (2021).
[48] M. Hatlo, F. James, P. Mato, L. Moneta, M. Winkler, and A. Zsenei, IEEE Trans. Nucl. Sci. **52**, 2818 (2005).
[49] S. Navas *et al.* (Particle Data Group), Phys. Rev. D **110**, 030001 (2024).
[50] U. G. Meißner, J. Ruiz de Elvira, M. Hoferichter, and B. Kubis, EPJ Web Conf. **137**, 01014 (2017).